

# Fin-Width Dependence of BJT-Based 1T-DRAM Implemented on FinFET

Dong-II Moon, Sung-Jin Choi, Jin-Woo Han, Sungho Kim, and Yang-Kyu Choi

**Abstract**—This letter investigates fin-width dependence on single-transistor latch (STL) for bipolar-junction-transistor (BJT)-based 1T-DRAM through experiments. The minimum drain voltage ( $V_{latch}$ ) for the activation of a parasitic lateral BJT in SOI FinFET was measured at various gate lengths ( $L_G$ 's) and fin widths ( $W_{fin}$ 's). The multiplication factor and current gain of the parasitic BJT in SOI MOSFET are introduced as determinant factors. The experimental results clearly show that the value of  $V_{latch}$  is reduced in a shorter  $L_G$  and wider  $W_{fin}$  device. It was found that the nonlocal effect retards the reduction of  $V_{latch}$  as FinFET scales down.

**Index Terms**—Bipolar-junction-transistor (BJT)-based 1T-DRAM, capacitorless 1T-DRAM, DRAM, embedded memory, FinFET, nonlocal effect, parasitic BJT, single-transistor latch (STL), SOI MOSFET.

## I. INTRODUCTION

A CAPACITORLESS 1T-DRAM based on a parasitic lateral bipolar-junction-transistor (BJT) in SOI MOSFET has been proposed to improve data retention time and current sensing margin [1]. It was also considered as an alternative for conventional DRAM [1]–[3]. Due to the absence of an external capacitor, 1T-DRAM is very attractive for embedded memory and miniaturization of a cell size. To extend the 1T-DRAM roadmap for future DRAM generations, a 1T-DRAM based on FinFET has been introduced [4]. As the gate length ( $L_G$ ) is scaled down, the fin width ( $W_{fin}$ ) tends to be reduced accordingly to suppress the short-channel effects (SCEs). One of the most remarkable virtues of the BJT-based 1T-DRAM compared with other 1T-DRAM operations lies in the aggressive scaling of the 1T-DRAM cell because a partially depleted body to increase the channel volume is not necessary. This indicates that the BJT-based 1T-DRAM shows supreme performance, even in a fully depleted (FD) SOI device on account of its unique physical mechanism: the single-transistor latch (STL) phenomenon [5]. The minimum drain voltage ( $V_D$ ) to trigger STL, namely, latch voltage ( $(V_{latch})$ ), is a key parameter because it enables

the BJT-based 1T-DRAM. The effect of  $L_G$  scaling on  $V_{latch}$  for the BJT-based 1T-DRAM is well understood [3]. However, a study of  $W_{fin}$  dependence on  $V_{latch}$  for the BJT-based 1T-DRAM has not yet been undertaken. There have been a few studies on BJT-based 1T-DRAM, but the  $W_{fin}$  dependence has not yet been adequately analyzed [4], [6]. Therefore, the study of the correlation between  $V_{latch}$  and  $W_{fin}$  in FinFET for the BJT-based 1T-DRAM is timely and essential.

In this letter, SOI FinFETs were fabricated, and  $W_{fin}$  dependence on STL was investigated to provide physical insights on the BJT-based 1T-DRAM.  $V_{latch}$  with various  $W_{fin}$ 's was measured, and a numerical simulation was performed to verify the effects on STL with  $W_{fin}$  reduction.

## II. RESULTS AND DISCUSSION

The device fabrication procedures and device characteristics for the FD SOI FinFET were described in our previous work [7], except for the formation of the diffused p-n junction S/D. All simulations were performed using ATLAS from SILVACO [8]. In this simulation, the FinFET had 300-nm  $L_G$  with 10-nm EOT, undoped fin, abrupt S/D junctions, and n<sup>+</sup> polysilicon gates, which were extracted from the fabricated device.

Fig. 1(a) shows the measured STL characteristics. At low  $V_D$ , the FinFET shows normal transfer behaviors. If the value of  $V_D$  is further increased, the subthreshold slope ( $S$ ) becomes very steep, i.e.,  $S < 10$  mV/dec. Also, the hysteresis loop develops. At this point, substantial impact ionization activates the parasitic BJT, which leads to STL. The transistor remained in the latch state without an inverted channel ( $V_G < V_T$ ) as long as the high  $V_D$  was maintained. It should be noted that the unique hysteresis loop can be utilized as a memory device. As a consequence, Fig. 1(b) shows the capacitorless 1T-DRAM operation based on the BJT method [1]–[4]. The measured characteristics of the BJT-based 1T-DRAM show a large current sensing margin and excellent retention properties without degradation via the positive feedback mechanism [6].

To investigate the relationship between the device scaling and the STL condition,  $V_{latch}$  was measured for two parameters:  $L_G$  and  $W_{fin}$ . Fig. 2 shows  $V_{latch}$  versus  $L_G$  and  $W_{fin}$ .  $V_{latch}$  is reduced as  $L_G$  is scaled down, but is increased as  $W_{fin}$  is narrowed. These results can be explained by referring to the  $I_D$  model for SOI MOSFET devices [5]

$$I_D = \frac{M \cdot I_{Ch}}{1 - \beta(M - 1)} \quad (1)$$

$$M - 1 = \frac{A_i}{B_i} (V_D - V_{Dsat}) \cdot \exp \left[ -\frac{B_i \lambda}{V_D - V_{Dsat}} \right] \quad (2)$$

Manuscript received May 9, 2010; revised May 25, 2010; accepted May 25, 2010. Date of publication July 19, 2010; date of current version August 25, 2010. This work was supported by a National Research Foundation (NRF) grant funded by the Korea government (K20901000002-09E0100-00210), by the IT R&D program of MKE/KEIT (10029953, Terabit Nonvolatile Memory Development), and was supported in part by the Nano R&D program through the National Research Foundation of Korea funded by the Ministry of Education, Science and Technology under Grant 2009-0082583. The review of this letter was arranged by Editor X. Zhou.

The authors are with the Department of Electrical Engineering, Korea Advanced Institute of Science and Technology, Daejeon 305-701, Korea (e-mail: ykchoi@ee.kaist.ac.kr).

Color versions of one or more of the figures in this letter are available online at <http://ieeexplore.ieee.org>.

Digital Object Identifier 10.1109/LED.2010.2052015

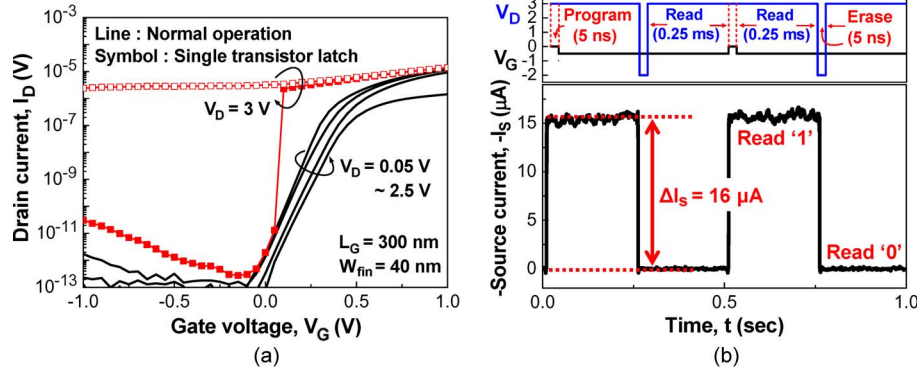


Fig. 1 (a) Characteristics of  $I_D$  versus  $V_G$  for various drain voltages. At low  $V_D$  from 0.05 to 2.5 V, the device shows normal operation. At  $V_D = 3$  V, the parasitic BJT is abruptly turned on, and bistable operation is enabled during (filled symbol) forward and (hollow symbol) reverse scans. (b) Measured results of the BJT-based 1T-DRAM. The operational biases are depicted in the upper side. In programming,  $V_G$  and  $V_D$  are set to 0 and 3 V, respectively. In reading,  $V_G$  is set to  $-0.5$  V, but  $V_D$  is not changed. The required  $V_D$  for programming and reading the 1T-DRAM cell is identical to  $V_{latch}$ . During erase operation, the forward p-n junction current is utilized. The current sensing margin ( $\Delta I_S$ ) is 16  $\mu$ A from an  $L_G$  of 300 nm and a  $W_{fin}$  of 40 nm.

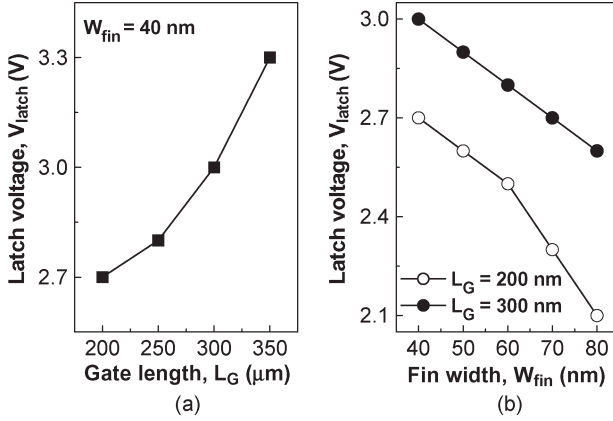


Fig. 2 (a)  $V_{latch}$  versus  $L_G$ . The increase in both  $M$  and  $\beta$  contributes to the lowering of the value of  $V_{latch}$  at a shorter  $L_G$ . (b)  $V_{latch}$  versus  $W_{fin}$ . The value of  $V_{latch}$  increased as  $W_{fin}$  was reduced resulting from the decrease in both  $M$  and  $\beta$ .

where  $M$  is the multiplication factor of the SOI MOSFET,  $I_{ch}$  is the MOSFET channel current, and  $\beta$  is the current gain of the parasitic lateral BJT.  $M$  is expressed by (2) [9].  $A_i$  and  $B_i$  are the process-dependent impact ionization constants, and  $\lambda$  is the characteristic length. From (1), the abnormal increase of  $I_D$  appears as  $\beta(M - 1)$  approaches unity. That is, STL is determined by the combination of  $M$  and  $\beta$ . In an FD SOI MOSFET, an  $L_G$  corresponding to a base width in the BJT primarily impacts  $\beta$  [10]. As  $L_G$  is decreased, it is obvious that the base width of the lateral BJT is decreased and  $\beta$  is increased by  $1/L_G$ . Even though the dependence of  $L_G$  on  $M$  is not shown explicitly in (2),  $M$  is increased as  $L_G$  is decreased due to the higher electric field. The increase in both  $M$  and  $\beta$  contributes to a lowering of  $V_{latch}$  at the decreased  $L_G$ , as shown in Fig. 2(a). The impact of  $L_G$  on STL can be well understood, and its result from FinFET is consistent with a trend shown in a previous planar SOI MOSFET.  $M$  depends heavily on  $B_i$ , and  $B_i$  was refined to apply the FinFET structure, which includes nonlocal carrier heating [9]

$$B_i = B_0 \left( 1 + \frac{\lambda_e}{\lambda} \right) \quad (3)$$

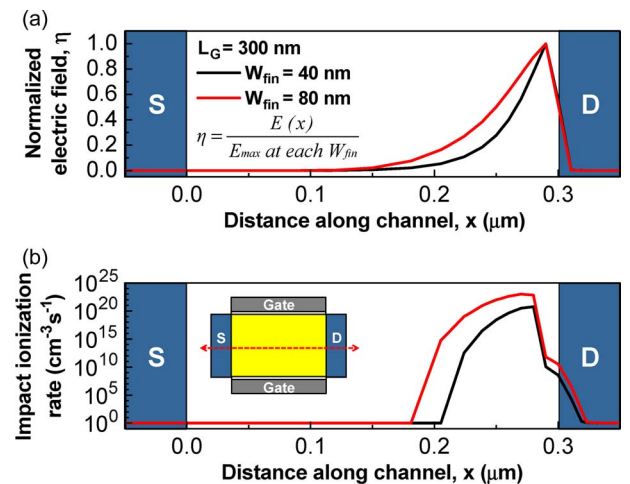


Fig. 3 Numerically simulated results of two different  $W_{fin}$  devices. (a) Electric field distribution along the channel at the middle of the fin. The electric field is normalized by the maximum lateral electric field for each  $W_{fin}$ . The lateral electric field varies more rapidly at the narrower  $W_{fin}$ . (b) Impact ionization rate along the channel at the middle of the fin. The impact ionization rate is decreased at the narrowed  $W_{fin}$  due to the nonlocal effect.

where  $B_0$  is the impact ionization constant and  $\lambda_e$  is the energy relaxation length. As the device scales down, the energy of the electrons lags behind the electric field under the rapidly increasing electric field, namely, the nonlocal effect [11]. As  $W_{fin}$  is decreased,  $M$  is greatly reduced due to the nonlocal effect. In addition, the accumulation of excess holes in the bulk region deactivates the parasitic BJT at the surface of the reduced  $W_{fin}$  [6]. Therefore, the narrow  $W_{fin}$  suppress STL, as shown in Fig. 2(b).

A numerical simulation to support the  $W_{fin}$  effect on STL was carried out by the use of two different  $W_{fin}$  cases. In this simulation,  $V_G$  and  $V_D$  were fixed at the STL condition of the 80-nm  $W_{fin}$  device. Fig. 3(a) shows the simulated results for the normalized lateral electric field at the middle of the fin. In contrast with the 80-nm  $W_{fin}$  case, the lateral electric field varies more rapidly at the 40-nm  $W_{fin}$ . The rapid spatial variation in electric field prevents carriers from reaching a steady-state equilibrium with the local electric field, and the electron temperature of the narrowed  $W_{fin}$  is reduced. Although

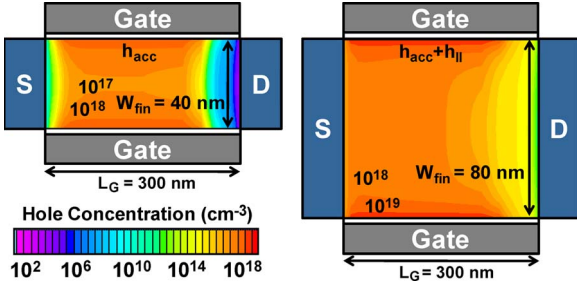


Fig. 4 Simulated hole concentrations after programming. The devices are biased in the read condition of the BJT-based 1T-DRAM. More holes are found underneath the interface of the gate oxide and channel at the 80-nm fin-width device because additional holes ( $h_{II}$ 's) generated by impact ionization are added to the preexisting accumulated holes ( $h_{acc}$ 's). In the center of the floating-body, excess hole concentration is consistently higher in the 80-nm device than that in the 40-nm device.

the maximum electric field on the drain side is increased as  $W_{fin}$  is reduced, the impact ionization rate of the narrow  $W_{fin}$  device is reduced [12]. The different impact ionization rates between the narrow and wide  $W_{fin}$ 's of Fig. 3(b) implies a retarded energy gain due to the nonlocal effect. The simulation results clearly indicate that the impact ionization rate is reduced as  $W_{fin}$  is narrowed. Therefore, the holes that trigger the parasitic BJT operation are not generated sufficiently due to the decrease of the impact ionization rate in the narrow  $W_{fin}$  device. That is, the value of  $V_D$  required for the operation of the BJT-based 1T-DRAM increases as  $W_{fin}$  is reduced.

The simulated hole concentrations of the two different  $W_{fin}$  devices are shown in Fig. 4. In the wide- $W_{fin}$  case, excess holes are charged under the gate oxide as a result of capacitive coupling. The different hole concentrations can be explained by the different impact ionization rates in Fig. 3(b). The BJT-based 1T-DRAM operation is determined by the existence of additional holes in the floating-body. It should be noted that the memory operation with a scaled FinFET is severely affected by  $W_{fin}$  reduction. However,  $V_{latch}$  is not effectively reduced as the device is scaled down. According to the simple scaling theory, the minimum  $L_G$  that suppresses SCEs is approximately twice that of  $W_{fin}$  [13]. If the value of  $W_{fin}$  is less than  $L_G/2$ , the BJT-based 1T-DRAM cannot satisfy the STL conditions due to nonlocal effects and the bulk-accumulation effect [6]. On the other hand, if the device has a wide  $W_{fin}$ , the current sensing margin of the BJT-based 1T-DRAM can approach zero due to the high leakage current [14]. Therefore,  $W_{fin}$  should be carefully designed for reliable memory operation.

### III. CONCLUSION

Fin-width dependence on STL has been investigated for the BJT-based 1T-DRAM built on FinFET. To analyze the effects

of device scaling on the BJT-based 1T-DRAM, the activation voltage of an STL was measured at various gate lengths and fin widths. Whereas the shorter gate length allowed the reduction of the latch voltage, the narrower fin width acted conversely on the latch voltage, i.e., increment of the latch voltage. From the numerical simulation, it was discerned that the nonlocal effect was a distinct feature of the suppression of impact ionization in the narrow fin width, which adversely led to increments of the latch voltage.

### REFERENCES

- [1] S. Okhonin, M. Nagoga, E. Carman, R. Beffa, and E. Faraoni, "New generation of Z-RAM," in *IEDM Tech. Dig.*, Dec. 2007, pp. 925–928.
- [2] K.-W. Song, H. Jeong, J.-W. Lee, S. I. Hong, N.-K. Tak, Y.-T. Kim, Y. L. Choi, H. S. Joo, S. H. Kim, H. J. Song, Y. C. Oh, W.-S. Kim, Y.-T. Lee, K. Oh, and C. Kim, "55 nm capacitor-less 1T DRAM cell transistor with non-overlap structure," in *IEDM Tech. Dig.*, Dec. 2008, pp. 797–800.
- [3] T.-S. Jang, J.-S. Kim, S.-M. Hwang, Y.-H. Oh, K.-M. Rho, S.-J. Chung, S.-O. Chung, J.-G. Oh, S. Bhardwaj, J. Kwon, D. Kim, M. Nagoga, Y.-T. Kim, S.-Y. Cha, S.-C. Moon, S.-W. Chung, S.-J. Hong, and S.-W. Park, "Highly scalable Z-RAM with remarkably long data retention for DRAM application," in *VLSI Symp. Tech. Dig.*, Jun. 2009, pp. 234–235.
- [4] S. Okhonin, M. Nagoga, C.-W. Lee, J.-P. Colinge, A. Afzalian, R. Yan, N. Dehdashti Akhavan, W. Xiong, V. Sverdlov, S. Selberherr, and C. Mazure, "Ultra-scaled Z-RAM cell," in *Proc. IEEE Int. SOI Conf.*, Oct. 2008, pp. 157–158.
- [5] J. Y. Choi and J. G. Fossum, "Analysis and control of floating-body bipolar effects in fully depleted submicrometer SOI MOSFETs," *IEEE Trans. Electron Devices*, vol. 38, no. 6, pp. 1384–1391, Jun. 1991.
- [6] Z. Zhou, J. G. Fossum, and Z. Lu, "Physical insights on BJT-based 1T DRAM cells," *IEEE Electron Device Lett.*, vol. 30, no. 5, pp. 565–567, May 2009.
- [7] S.-J. Choi, J.-W. Han, S. Kim, D.-H. Kim, M.-G. Jang, J.-H. Yang, J. S. Kim, K. H. Kim, G. S. Lee, J. S. Oh, M. H. Song, Y. C. Park, J. W. Kim, and Y.-K. Choi, "High speed flash memory and 1T-DRAM on dopant segregated Schottky barrier (DSSB) FinFET SONOS device for multi-functional SoC applications," in *IEDM Tech. Dig.*, 2008, pp. 223–226.
- [8] Silvaco, *Atlas User's Manual: Device Simulation Software*, Silvaco Int., Santa Clara, CA, 2008.
- [9] J.-W. Han, J. Lee, D. Park, and Y.-K. Choi, "Body thickness dependence of impact ionization in a multiple-gate FinFET," *IEEE Electron Device Lett.*, vol. 28, no. 7, pp. 625–627, Jul. 2007.
- [10] E. P. Ver Ploeg, C. T. Nguyen, S. S. Wong, and J. D. Plummer, "Parasitic bipolar gain in fully depleted n-channel SOI MOSFETs," *IEEE Trans. Electron Devices*, vol. 41, no. 6, pp. 970–977, Jun. 1994.
- [11] K. Taniguchi, M. Yamaji, K. Sonoda, T. Kunikiyo, and C. Hamaguchi, "Monte Carlo study of impact ionization phenomena in small geometry MOSFETs," in *IEDM Tech. Dig.*, Dec. 1994, pp. 355–358.
- [12] C.-W. Lee, A. Afzalian, R. Yan, N. Dehdashti Akhavan, W. Xiong, and J.-P. Colinge, "Drain breakdown voltage in MuGFETs: Influence of physical parameters," *IEEE Trans. Electron Devices*, vol. 55, no. 12, pp. 3503–3506, Dec. 2008.
- [13] K. Suzuki, T. Tanaka, Y. Tosaka, H. Horie, and Y. Arimoto, "Scaling theory for double-gate SOI MOSFETs," *IEEE Trans. Electron Devices*, vol. 40, no. 12, pp. 2326–2329, Dec. 1993.
- [14] S.-J. Choi, J.-W. Han, D.-I. Moon, and Y.-K. Choi, "Analysis and evaluation of a BJT-based 1T-DRAM," *IEEE Electron Device Lett.*, vol. 31, no. 5, pp. 393–395, May 2010.